Optics Letters

High-performance GaN-based green resonant cavity-light emitting diodes with an Ag bottom mirror

Mingshuang Ma,[1] Shuai Yang,[2,5] Leiying Ying,[1] Yikun Bu,[3] Yang Mei,[1,6] and Baoping Zhang[1,4,*]

[1]Laboratory of Micro/Nano-Optoelectronics, Department of Micro Electronic and Integrated Circuits, Xiamen University, Xiamen 361005, China
[2]Institute of Advanced Displays and Imaging, Henan Academy of Sciences, Zhengzhou, 450016, China
[3]Laboratory of Optical Thin Film Materials and Devices, Department of Micro Electronic and Integrated Circuits, Xiamen University, Xiamen 361005, China
[4]Institute of Nanoscience and Applications (INA), Southern University of Science and Technology (SUSTech), Shenzhen, 518055, China
[5]yangshuai@hnas.ac.cn
[6]meiyang@xmu.edu.cn
*zhangbp@sustech.edu.cn

Received 28 January 2025; revised 4 March 2025; accepted 28 March 2025; posted 1 April 2025; published 14 April 2025

Green resonant cavity light-emitting diodes (RCLEDs) are important components in optical communication and display applications. However, the light output power (LOP) is usually limited. In this study, GaN-based green RCLEDs with a large chip size ($900 \times 900\ \mu m^2$) have been fabricated using a silver (Ag) metal mirror as the bottom reflector and a dielectric distributed Bragg reflector (DBR) as the top reflector. The device is characterized by a small spectral linewidth (3.0 nm) and divergence angle (95°) when compared with standard LEDs, which is attributed to the cavity effect. The turn-on voltage is 2.3 V at an injection current of 20 mA, with a LOP of 180 mW at a current density of 197 A/cm^2, which is the highest LOP reported to date for green RCLEDs. The Ag bottom mirror can not only enhance the cavity effect but also improve heat dissipation and electrical injection. The utilization of array configuration for the n-side electrode has not only enabled uniform current injection but has also maximized the light output area that contributes to the high LOP. © 2025 Optica Publishing Group. All rights, including for text and data mining (TDM), Artificial Intelligence (AI) training, and similar technologies, are reserved.

https://doi.org/10.1364/OL.558166

Gallium nitride (GaN) is an effective direct bandgap semiconductor that exhibits good optoelectronic performance with an adjustable bandgap from 0.7 to 6.28 eV [1]. The GaN emission wavelength spans the infrared and ultraviolet range, and GaN-based materials are widely employed in optoelectronic applications. Gallium nitride-based blue and green LEDs provide full-spectrum illumination and full-color displays, with potential applications in visible light [2] and underwater optical communications. Moreover, plastic optical fibers (POF) based on polymethyl methacrylate (PMMA) are suitable for short-distance data transmission using green light as PMMA has a low-loss window in the green wavelength band [3].

Advances in material epitaxial growth and device development have served to significantly increase the internal quantum efficiency of LEDs. However, the extraction efficiency is limited by the total reflection critical angle [4], and a small proportion of photons are emitted from the surface. Surface roughening and the use of transparent substrates, tilted interfaces, and resonant cavity structures have been employed to enhance photon extraction efficiency [5]. LEDs have a large emission divergence angle, a high associated full width at half the maximum (FWHM) emission, and low spectral purity. The application of a resonant cavity structure to form a RCLED can address some of these issues [6]. However, RCLEDs usually exhibit a lower light output power. In the green spectral region, large lattice-mismatch may cause defects which act as non-radiative recombination centers. In addition, the polarization induced electric field results in a strong quantum confinement Stark effect (QCSE). These issues collectively lead to a sharp decrease in the luminescence efficiency of InGaN quantum wells in the green wavelength band [7]. Apart from these issues associated with material growth, there are also some special issues of RCLED related with fabrication process, device structure, etc. There has been a concerted research effort to improve device performance, such as weakening the QCSE, using patterned substrates [8–10], and optimizing the structure of the resonant cavity. Since the inception of the resonant cavity light-emitting diode (RCLED) concept based on the Fabry–Perot (FP) cavity principle by Schubert *et al.* in1992 [11], RCLEDs have experienced rapid development owing to their significant advantages. Subsequently, continuous efforts have been dedicated to optimize the resonant cavity structure to enhance device performance. In 2000, RC^{2}LED (Resonance Behavior Reflector, RCR) was proposed by Peter Bienstman to improve light extraction, achieving narrower linewidth and higher extraction efficiency [12]. In 2003, Ghawana *et al.* integrated a grating-assisted (GA) structure into RCLEDs, significantly increasing the LOP [13]. In 2009, Munnix *et al.* fabricated quantum dot micro-cavity (QD-MC) LEDs using the metal organic chemical vapor deposition (MOCVD), which further elevated the LOP of the devices [14]. To a certain extent, the structural optimizations of the resonant cavity have consistently contributed to the improvement of the LOP of RCLEDs. In 2002, Maaskant *et*

al. used a Pd/Ag metal bottom mirror and AlGaN/GaN top reflector to prepare green RCLEDs with an emitting wavelength of 510 nm, a FWHM of 28 nm, and a maximum LOP of 0.33 mW [15]. However, the nitride DBR exhibited a narrow high reflective band, and the associated growth procedure is complex and costly. In 2006, Huang *et al.* reported a GaN-based green RCLED, fabricated by combining a Ni/Ag bottom mirror and five pairs of TiO_2/SiO_2 top DBR on a silicon substrate. The FWHM was reduced to 5.5 nm with a LOP of 0.17 mW [16]. In 2008, Huang *et al.* prepared green RCLEDs with Ti/Al bottom mirrors and three pairs of TiO_2/SiO_2 top dielectric DBR. The size of the device was $356 \times 356\ \mu m^2$, with a luminescence center at 507 nm and a maximum LOP of 1.06 mW [17]. The above devices all featured a lateral current injection, which causes current crowding and a thermal effect at high current [18], limiting the device LOP. In 2020, Wu *et al.* reported a GaN-based flip-chip vertical structured green RCLED. The device LOP was enhanced by employing vertical current injection and gradient trapezoidal quantum wells. Using the dielectric DBRs and Ag mirrors as the top and bottom reflectors, respectively, the RCLEDs achieved a LOP of 115 mW at a current density of 210 A/cm^2 and a FWHM of 6.4 nm [19]. Although the flip-chip structure improved the thermal performance of the device, the bonding process is complicated [20]. In our previous work, vertically structured green RCLEDs with a LOP of 11.1 mW at a current density of 50 A/cm^2 and FWHM of 14 nm were fabricated. The cavity was formed by the combination of a bottom Al mirror and a top dielectric DBR. The epitaxial material was grown on a patterned sapphire substrate (PSS) to improve crystal quality, and the device was mounted on a Cu substrate by electrical plating to improve thermal dissipation [21]. The device exhibited an enhanced performance, but further improvements are required.

In this study, we have adopted a high reflectivity Ag mirror as the bottom reflector (p-side), with a combination of top dielectric DBRs (n-side). The Ag side is bonded to a conductive Si substrate, which facilitates heat dissipation. The n-electrode structure has been optimized in order to enhance the effective light-emitting area of the device (~86.6%) and increase the light output power. In the device with two pairs of top DBR, a very high LOP (180 mW at a current density of 197 A/cm^2), a lower turn-on voltage (~2.3 V at 20 mA), a smaller FWHM (3.0 nm), and a smaller divergence angle (95°) were achieved.

A low-pressure metal organic chemical vapor deposition (MOCVD) system was used to grow green optical epitaxial layer materials on a c-plane PSS. A low-temperature nucleated GaN layer with a thickness of 5 nm was grown on the PSS, followed by the growth of a 3 μm undoped GaN (u-GaN) layer and the deposition of a 3 μm Si-doped n-GaN. Subsequently, 15 pairs of high In-component green-emitting $In_{0.25}Ga_{0.75}N/GaN$ (3 nm/12 nm) quantum wells were deposited, followed by the growth of a 30 nm electron blocking layer (AlGaN). Finally, a 700 nm Mg-doped p-GaN layer was grown.

For the selection of metal mirrors, four commonly used metals (Ag, Al, Cu, and Au) were evaluated [22]. As shown in Fig. 1, Ag exhibits the best performance in terms of reflectance in the green band while also delivering better electrical and thermal conductivity. Consequently, Ag was chosen as the lower reflector, enhancing the resonance cavity effect, with superior conductivity and effective thermal dissipation. These features contribute to enhanced device performance, enabling operation at higher current and higher power.

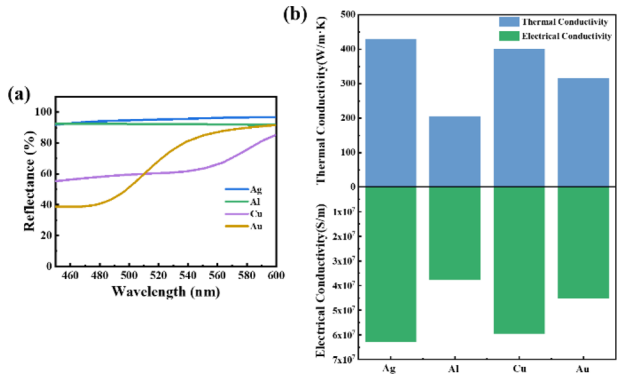

Fig. 1. (a) Reflectance of different metallic materials in the green light band. (b) Thermal and electrical conductivity of selected metals at room temperature.

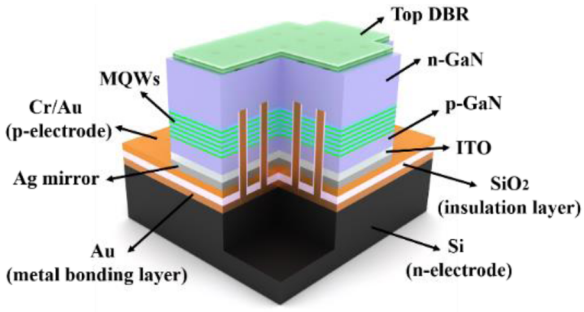

Fig. 2. Schematic representation of the device structure.

The structure of the device is illustrated in Fig. 2. The cross section of the device structure and the detailed process flow are shown in Figs. S1 and S2 in Supplement 1. The Ni/Ag (1/90 nm) metallic reflector was first deposited on the indium tin oxide (ITO) film by magnetron sputtering and serves as the bottom reflector. Then, by employing photolithography and magnetron sputtering techniques, a patterned Cr/Au layer is constructed as a p-electrode. Uniformly distributed holes of 60 μm diameter were etched, reaching the n-GaN layer, using photolithography and inductively coupled plasma (ICP) techniques. The experimental parameters for the ICP etching of GaN for the device fabrication are shown in Table S1 in Supplement 1. And the SiO_2 insulation layer (1 μm) was deposited by means of magnetron sputtering to preclude short circuits. Subsequently, a metal bonding layer was formed on the entire surface by magnetron sputtering, and the sample was flipped and bonded to an n-type conductive silicon substrate, which served as the n-electrode. The patterned sapphire substrate was then removed by laser lift off (LLO), followed by chemical mechanical polishing (CMP) to reduce the layer thickness and flatten the surface. Afterward, photolithography and ICP technology were utilized to separate the device stages. Finally, electron beam evaporation was used to deposit the TiO_2/SiO_2 dielectric DBR as the upper reflector, completing the device fabrication (see Supplement 1, Figs. S3 and S4).

In fabricating the RCLEDs, we selected configurations with two, three, and six pairs of DBRs as the top reflector and the Ag mirror as the bottom reflector. The electroluminescence (EL) spectra of devices with two, three, and six pairs of DBRs were determined at varying injection currents, as shown in Fig. 3. It

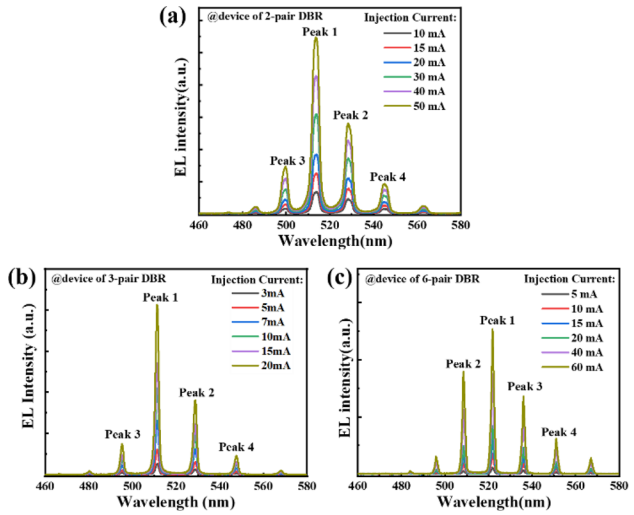

Fig. 3. Electroluminescence spectra (a) two-pair DBR, (b) three-pair DBR, and (c) six-pair DBR.

can be seen from Figs. 3(a)–3(c) that the luminescence intensity increased with increasing injection current. Each device demonstrated multimode luminescence, and the emission peaks remained stable with varying injection current. The FWHM of the main light-emitting peak fell from 3.0 nm for two-pair DBR to 1.6 nm for three-pair DBR and 1.3 nm in the case of six-pair DBR. The FWHM decreased as the number of DBR pairs was increased. This variation is due to the increased reflectivity of the DBR (see Supplement 1, Fig. S4). By increasing the reflectivity of the top reflector, the probability of photon reflection in the resonance cavity is increased, promoting the resonance cavity effect [23,24]. Ultimately, this results in a decrease in the spectral linewidth of the RCLED with enhanced purity of the luminescence.

In order to further investigate the optoelectronic performance of different numbers of pairs of DBRs, the LOP was tested. The associated LOP was determined using a spectrometer with an integral sphere allowing measurements under a continuous wave current at room temperature. The results are presented in Fig. 4(a), where it can be seen that the device LOP decreased with an increase in the number of DBR pairs. The LOP of the device with two-pair DBR reached a maximum of 147.2 mW at 125 A/cm^2. Increasing the number of DBR pairs to three resulted in a drop of the LOP to 98.6 mW with a further decrease to 69.1 mW, with six pairs. The latter value is less than half that recorded for the device with two-pair DBR. This response can be attributed to an increase in reflectivity as the number of DBR pairs is increased. More of the emitting light is reflected back into the cavity, leading to photon reabsorption and recycling in the multi-quantum well (MQW). Only the light that oscillates in the cavity mode contributes to the LOP. Furthermore, the increased reflectivity also generates additional internal total reflection and Fresnel losses [25], and combining Fig. 3, it can be observed that although the FWHM decreases as the number of DBR pairs and the reflectivity increase, it concurrently leads to a reduction in the LOP of the device. The dependence of LOP on injection current in the case of the device with two-pair DBR was examined under a higher current density, as shown in Fig. 4(b). The device LOP reached a value of 180 mW at 197 A/cm^2, which represents the highest recorded value for green RCLEDs.

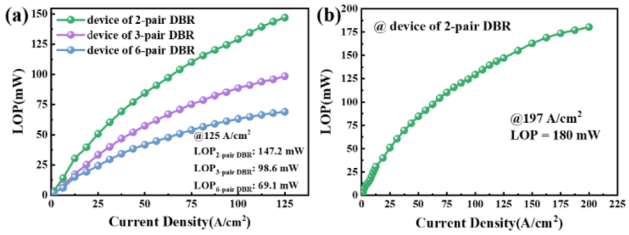

Fig. 4. Light output power for different numbers of pairs of DBRs.

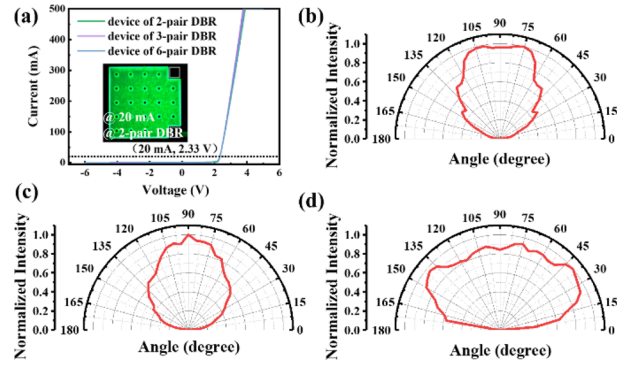

Fig. 5. (a) I–V characteristics of the RCLED with different numbers of pairs of DBRs (the inset shows the actual luminescence of the device with two-pair DBR at an injection current of 20 mA). Far-field divergence angle for the devices with (b) two-pair DBR, (c) three-pair DBR, and (d) six-pair DBR.

The I–V characteristics of the three devices are shown in Fig. 5(a). The devices all exhibited a relatively low turn-on voltage (~2.3 V) at an injection current of 20 mA. The low turn-on voltage can result from the release of residual stresses in the epitaxial layer after LLO, which reduces the barrier height and energy band tilt, enhancing the efficiency of carrier injection into the quantum well [26]. Moreover, the optimization of the n-electrode structure improves the efficiency and homogeneity of the injected carriers. Taking the device with two-pair DBR as representative, the emission was uniform under an injection current of 20 mA, as shown in the inset of Fig. 5(a). To examine the low-current regime in more detail, a semi-logarithmic scale was applied to the current axis, as shown in Supplement 1 (Fig. S5).

The far-field distribution of RCLEDs determines the efficiency of coupling with optical fibers [9]. This is evaluated in Figs. 5(b)–5(d), where the RCLED divergence angles are shown for different numbers of DBR pairs at 20 mA. The far-field half-intensity angles of the RCLEDs with two, three, and six pairs of top DBRs are 95, 103.5, and 163°, respectively. When the resonant cavity structure is introduced, the far-field divergence angle is narrower, indicating an enhanced directionality of the emission spectrum [24]. However, an increase in the number of DBR pairs (to six) served to increase the divergence angle, and the luminous intensity was largely unchanged within the 20–160° range. This is because, as the number of DBR pairs increases, the top DBR with high reflectivity suppresses more the light emission, and the lower transmittance of the six-pair DBR in the vertical direction leads to a wider divergence angle. Therefore, the top DBR with moderate reflectivity can more effectively improve the directionality of the emission spectrum compared to a DBR with high reflectivity, allowing more photons to escape through the extraction cone [24].

In this study, high-power green GaN-based RCLEDs were fabricated with a bottom Ag reflector and a top dielectric DBR. The properties of devices with a different number of top DBR pairs have been compared. Compared with a vertical LED without cavity, the optoelectronic performance of this device has been significantly improved (see Supplement 1, Fig. S6). The device with two-pair DBR exhibited a high light output power (180 mW at 197 A/cm^2), a low turn-on voltage (~2.3 V at 20 mA), a narrow FWHM (3.0 nm), and a small far-field divergence angle (95°). The light output power is significantly higher than the values reported for green RCLEDs. The epitaxial growth of the wafer on a PSS substrate serves to improve the crystal quality. The array-format arrangement of the n-side electrode improves the homogeneity of the electrical injection. The metal Ag mirror employed as the bottom reflector enables high reflectivity and good electrical and thermal conductivity. The results provide useful reference for high performance GaN-based RCLEDs.

Funding. National Natural Science Foundation of China (U21A20493, 62234011).

Disclosures. The authors declare no conflicts of interest.

Data availability. Data underlying the results presented in this Letter are not publicly available at this time but may be obtained from the authors upon reasonable request.

Supplemental document. See Supplement 1 for supporting content.

REFERENCES

1. M. Leroux, S. Dalmasso, F. Natali, *et al.*, Phys. Status Solidi B **234**, 887 (2002).
2. F. M. Wu, C. T. Lin, C. C. Wei, *et al.*, IEEE Photonics J. **5**, 7901507 (2013).
3. L. Zhu, Z. Dong, J. Zou, *et al.*, Appl. Opt. **62**, 4102 (2023).
4. S. Chichibu, T. Azuhata, T. Sota, *et al.*, Appl. Phys. Lett. **69**, 4188 (1996).
5. R. Windisch, C. Rooman, S. Meinlschmidt, *et al.*, Appl. Phys. Lett. **79**, 2315 (2001).
6. D. Delbeke, R. Bockstaele, P. Bienstman, *et al.*, IEEE J. Sel. Topics Quantum Electron. **8**, 189 (2002).
7. J. Cho, E. Schubert, and J. K. Kim, Laser Photonics Rev. **7**, 408 (2013).
8. S. Zhou, Z. Wan, Y. Lei, *et al.*, Opt. Lett. **47**, 1291 (2022).
9. S. Zhou, X. Zhao, P. Du, *et al.*, Nanoscale **14**, 4887 (2022).
10. C. Xu, L. Cai, Z. Chen, *et al.*, Opt. Quantum Electron. **56**, 133 (2024).
11. E. F. Schubert, Y.-H. Wang, A. Y. Cho, *et al.*, Appl. Phys. Lett. **60**, 921 (1992).
12. P. Bienstman, IEEE J. Quantum Electron. **36**, 669 (2000).
13. K. Ghawana, D. Delbeke, I. Christiaens, *et al.*, SPIE **4947**, 25 (2003).
14. M. C. Munnix, A. Lochmann, D. Bimberg, *et al.*, IEEE J. Quantum Electron. **45**, 1084 (2009).
15. P. Maaskant, M. Akhter, B. Roycroft, *et al.*, Phys. Status Solidi B **192**, 348 (2002).
16. S.-Y. Huang, R.-H. Horng, W.-K. Wang, *et al.*, Jpn. J. Appl. Phys. **45**, 3433 (2006).
17. S. Y. Huang, R.-H. Horng, P. L. Liu, *et al.*, IEEE Photonics Technol. Lett. **20**, 797 (2008).
18. L. Zhu, Z. Ma, P. T. Lai, *et al.*, IEEE Trans. Electron Devices **58**, 490 (2011).
19. H. Wu, H. Li, S.-Y. Kuo, *et al.*, IEEE Trans. Electron Devices **67**, 3650 (2020).
20. S. Zhou, X. Liu, H. Yan, *et al.*, Opt. Express **27**, A669 (2019).
21. S. Yang, H. Xu, H. Long, *et al.*, Opt. Lett. **47**, 2858 (2022).
22. M. N. Polyanskiy, Sci. Data **11**, 94 (2024).
23. S. Zhao, B. Xu, Z. Zhao, *et al.*, Opt. Lett. **47**, 4616 (2022).
24. L. M. Zhou, B. C. Ren, Z. W. Zheng, *et al.*, ECS J. Solid State Sci. Technol. **7**, R34 (2018).
25. P.-H. Lei, S.-H. Wang, F. S. Juang, *et al.*, Opt. Commun. **283**, 1933 (2010).
26. Y. Pei, S. Zhu, H. Yang, *et al.*, Opt. Photonics J. **03**, 139 (2013).

110.63.147.157 2025-07-02 04:58:2